



Hydrophobic block copolymer ultrafiltration membranes for anti-scaling durable membrane distillation crystallization[☆]

Zhuo Li^a, Shoutian Qiu^{b,*}, Lei Wang^a, Kang Zhou^a, Shuda Liu^a, Yong Wang^{a,c,**} 

^a State Key Laboratory of Materials-Oriented Chemical Engineering, College of Chemical Engineering, Nanjing Tech University, Nanjing 211816 Jiangsu, PR China

^b College of Materials Science and Engineering, State Key Laboratory of Materials-Oriented Chemical Engineering, Nanjing Tech University, Nanjing 211816 Jiangsu, PR China

^c School of Energy and Environment, Southeast University, Nanjing 210096 Jiangsu, PR China

ARTICLE INFO

Editor: B. Van der Bruggen

Keywords:

Block copolymer
Membrane distillation crystallization
Anti-scaling
Selective swelling

ABSTRACT

Due to the inherent insensitivity to salt concentration, membrane distillation (MD) has emerged as a promising technology for high-salinity wastewater treatment. However, scaling remains a critical challenge hindering the widespread application of MD. This study proposes a solution through the development of triblock polystyrene-*block*-polydimethylsiloxane-*block*-polystyrene (SDS) membranes with precisely engineered pore structures that effectively address this limitation. The results demonstrate that controlled pore size reduction, which was achieved via selective swelling fabrication, significantly mitigates both surface scaling and intra-pore crystallization. The SDS membrane shows remarkable performance stability under diverse high-salinity conditions, including those high-salinity solutions containing common inorganic contaminants such as CaSO₄. Furthermore, when implemented in membrane distillation-crystallization (MDC), the SDS membrane maintains stable performance under a continuous operation for 168 h with saturated NaCl feed, successfully producing high-purity water while simultaneously recovering salt crystals. These results demonstrate that controlled pore size reduction represents an effective strategy to mitigate membrane scaling while maintaining performance stability, offering significant advantages for industrial implementation in zero liquid discharge systems treating high-salinity wastewater.

1. Introduction

The treatment of high-salinity wastewater is crucial for reducing environmental impact and recovering high-value resources [1,2]. However, conventional desalination methods such as multi-stage flush and reverse osmosis (RO) are inefficient in processing the extremely high salt content [3,4]. Membrane distillation (MD) technology offers a novel technical pathway for high-salinity wastewater treatment as a result of its unique advantages [5,6]. This process utilizes the vapor pressure difference across a hydrophobic porous membrane as the driving force, enabling volatile components from the feed side to permeate as gas molecules while achieving near-complete rejection of non-volatile components, with a theoretical salt rejection rate of 100% [7,8]. Unlike conventional thermal processes that typically require boiling temperatures, MD operates effectively at moderate temperatures

(40–80°C). This significantly lower thermal requirement enables efficient utilization of low-grade heat sources, including solar thermal energy and industrial waste heat streams [9,10]. Additionally, MD operates at much lower pressures (near 1 bar for vacuum MD) compared to RO which features salinity-dependent high operating pressures [11]. Moreover, since the driving force of MD depends on vapor pressure differential rather than osmotic pressure, its performance remains largely unaffected by feedwater salinity [12]. These characteristics position MD as a particularly suitable technology in achieving zero liquid discharge (ZLD) in applications of high-salinity wastewater treatment.

However, MD still faces the critical challenge of membrane scaling in practical applications [13,14]. In high-salinity environments, the supersaturated precipitation of salts on the membrane surface leads to severe scaling issues [15]. Firstly, crystal deposition blocks vapor transport channels and causes flux decline. Secondly, intra-pore

[☆] This article is part of a special issue entitled: 'Desalination technology' published in Separation and Purification Technology.

^{*} Corresponding author.

^{**} Corresponding author at: State Key Laboratory of Materials-Oriented Chemical Engineering, College of Chemical Engineering, Nanjing Tech University, Nanjing 211816, Jiangsu, PR China.

E-mail addresses: qiust@njtech.edu.cn (S. Qiu), yongwang@seu.edu.cn (Y. Wang).

<https://doi.org/10.1016/j.seppur.2025.133614>

Received 21 April 2025; Received in revised form 16 May 2025; Accepted 17 May 2025

Available online 21 May 2025

1383-5866/© 2025 Elsevier B.V. All rights are reserved, including those for text and data mining, AI training, and similar technologies.

crystallization compromises membrane structural integrity, triggering irreversible membrane wetting failure. Therefore, developing effective anti-scaling strategies is crucial for maintaining MD performance and extending operational lifespan.

To address this issue, current research primarily focuses on constructing superhydrophobic surfaces in reducing the liquid-membrane contact area, thereby minimizing the risk of heterogeneous nucleation [16–18]. By lowering surface energy and creating re-entrant structures, membrane surface hydrophobicity can be effectively enhanced. Wang and coworkers developed a highly superhydrophobic polyvinyl alcohol (PVA) membrane (the water contact angle is 157°) through a sophisticated fabrication process involving electrospinning, glutaraldehyde crosslinking, Al_2O_3 nanoparticle coating, and fluorination modification [19]. When treating coal gasification wastewater, the distillate conductivity remained below $6.74 \mu\text{S}\cdot\text{cm}^{-1}$. Tan *et al.* fabricated superhydrophobic nanofiber membranes with tailored membrane pore sizes via combined electrospinning and electrospaying approaches [20]. MD tests demonstrated that the increased evaporation area and reduced pore size could simultaneously mitigate the membrane scaling while enhancing flux. However, when treating CaSO_4 systems, severe gypsum scaling and pore blockage still occurred at a water recovery rate of 62%, leading to an abrupt flux decline.

The microporous structure of conventional MD membranes significantly increases the risk of intra-pore crystal nucleation and growth [21]. Through systematically investigating the effects of pore size, surface hydrophobicity, and porosity on wetting and scaling resistance, Allyson *et al.* found that reducing pore size and porosity proved more effective than merely enhancing the hydrophobicity [22]. Similarly, Gryta *et al.* demonstrated that a low-porosity surface layer could physically restrict crystal growth within pores, thereby significantly mitigating scaling-induced membrane wetting [22]. These findings provide new insights for MD membrane design: superior anti-scaling performance can be achieved by optimizing pore architecture rather than relying solely on surface modification [23]. However, excessive reduction in pore size and porosity may lead to severe flux decline, necessitating careful balance between pore structure regulation and permeate flux [24]. Wang *et al.* fabricated a dense layer on PVDF membranes using PVA and polyzwitterionic polymers to reduce pore size, thereby enhancing both wetting and scaling resistance [5,6]. The membrane maintained stable flux ($15\text{--}20 \text{ L}\cdot\text{m}^{-2}\cdot\text{h}^{-1}$) with exceptional rejection performance (conductivity $< 20 \mu\text{S}\cdot\text{cm}^{-1}$) in treating actual coal gasification wastewater.

Notably, MD and crystallization technologies exhibit inherent complementarity [25,26]: MD enables continuous feed solution concentration while the crystallization process reduces system supersaturation, thereby mitigating membrane scaling. This synergistic effect has given rise to the innovative membrane distillation-crystallization (MDC) process, providing an integrated solution for high-salinity wastewater treatment and resource recovery.

Our previous studies revealed that hydrophobic block copolymer membranes with ultrafiltration pore sizes demonstrate excellent anti-wetting performance even with moderate hydrophobicity (water contact angle $\sim 120^\circ$) [27]. The enhanced wetting-resistance is attributed to the small pore size and narrow pore size distribution. Block copolymers have the distinct benefit of enabling a narrow pore size distribution in membrane fabrication [28]. Selective swelling, an emerging pore generation approach, allows the minor block to form a porous structure without damaging structure integrity [29].

In this work, polystyrene-*block*-polydimethylsiloxane-*block*-polystyrene (PS-*b*-PDMS-*b*-PS, SDS) hydrophobic composite membranes were fabricated via the selective swelling process. The selective swelling process yielded an structure featuring high internal porosity coupled with low surface porosity. The vacuum membrane distillation (VMD) performance of thus-produced SDS composite membranes was systematically investigated under varying salinity conditions. The anti-scaling properties of the SDS membrane were evaluated by introducing

inorganic contaminants (CaSO_4) into feed solutions. Furthermore, the potential of the SDS membrane for MDC applications was explored by integrating a crystallization unit into the VMD system.

2. Experimental

2.1. Materials

The SDS copolymer was synthesized according to our previously work [27]. The experimental procedure involved two main steps: First, bis(aminopropyl)-functionalized PDMS was employed to prepare PDMS macroinitiators through a 48-h reaction. Subsequently, a predetermined quantity of the PDMS macroinitiator, styrene, and anhydrous tetrahydrofuran were introduced into a reaction vessel. The system was then degassed and vacuum-sealed before initiating the polymerization at 80°C for 24 h. This material contains PDMS segments with a molecular weight of 10 kDa, accounting for approximately 22% by mass. All chemicals were used as received: *n*-hexane ($\geq 95\%$) were purchased from Sigma-Aldrich. Chloroform ($\geq 99.0\%$) was supplied by Sinopharm Chemical. Absolute ethanol ($\geq 99.8\%$), sodium chloride (NaCl, $\geq 99.8\%$), sodium sulfate (Na_2SO_4 , $\geq 99.8\%$), and calcium chloride (CaCl_2 , $\geq 99.8\%$) were purchased from local suppliers. Hydrophilic polyvinylidene fluoride (PVDF) support membrane with a diameter of 47 mm and average pore size of 220 nm were purchased from Millipore and used as substrates. Deionized water with conductivity of $8\text{--}20 \mu\text{S}\cdot\text{cm}^{-1}$ was used for all tests.

2.2. Preparation of SDS composite membranes

The synthesized SDS copolymer was dissolved in chloroform to prepare a 2 wt% solution, which was then filtered through a 0.22 μm membrane filter for subsequent use. A 700 μL aliquot of SDS solution was deposited onto the hydrophilic PVDF substrate and spin-coated at 2000 rpm for 30 s to form a dense SDS layer. To prevent SDS solution penetration into the PVDF pores during coating, the PVDF substrates were pre-wetted by immersion in deionized water for 20 min, followed by careful removal of surface moisture prior to coating. The coated composite membranes were dried at room temperature for over 24 h. Subsequently, selective swelling was performed by immersing the SDS composite membranes in *n*-hexane at 25°C for 1 h, after which the samples were immediately removed and dried at ambient temperature for 24 h to allow complete solvent evaporation [27].

2.3. Characteristic

The membrane morphology was examined using field emission scanning electron microscopy (FESEM, Hitachi S4800) at an accelerating voltage of 3 kV. Prior to imaging, samples were sputter-coated with a thin platinum layer to enhance conductivity. To obtain clear cross-sectional views, membrane samples were cryogenically fractured in liquid nitrogen. Quantitative analysis of surface pore channels and diameter distribution was performed using the ImageJ software, while overall membrane porosity was calculated from the thickness variation before and after selective swelling.

The surface elemental distribution of the membrane after distillation test was characterized by energy-dispersive X-ray spectroscopy (EDS, Hitachi S-4800, Japan).

2.4. VMD and MDC tests

The separation performance of the SDS membrane was evaluated using a custom-built VMD system with an effective membrane area of 11.94 cm^2 , as illustrated in Fig. 1. The feed solution temperature was precisely controlled by a constant-temperature water bath, while a peristaltic pump maintained a circulation flow rate of $500 \text{ mL}\cdot\text{min}^{-1}$ through the membrane module. The permeate side was kept under 2

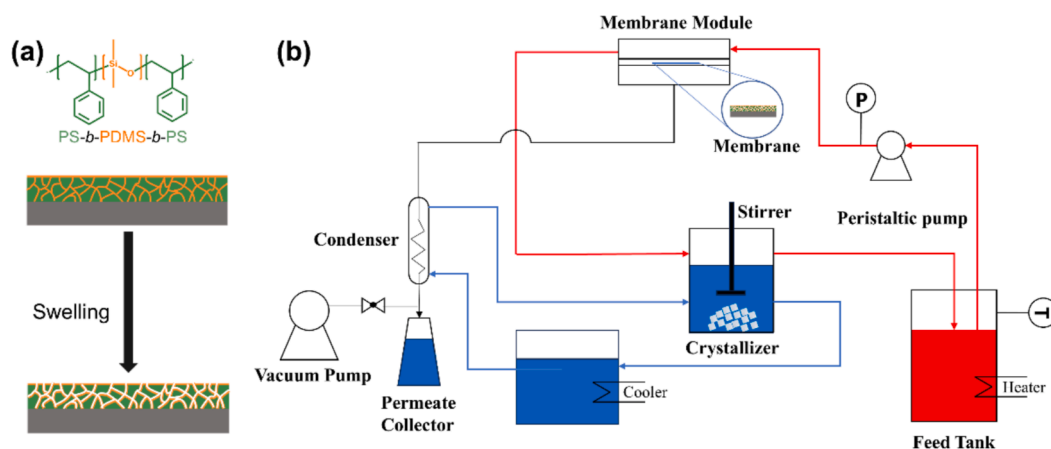


Fig. 1. (a) Schematic illustration of the membrane preparation processes by selective swelling of SDS. (b) Schematic diagram of MDC (red lines represent hot flows while blue lines represent cold flows).

kPa, with a condenser temperature maintained at 1°C to collect the distillate. Permeate mass and conductivity were continuously monitored using an electronic balance and conductivity meter, respectively. Various NaCl solutions (3.5, 5, 10, 15, 20 wt% and saturated solution at 25°C) were tested to simulate high-salinity wastewater. To evaluate the anti-scaling performance, the saturated CaSO₄ solution was prepared by adding 20 mM CaCl₂ and 20 mM Na₂SO₄ into the feed solution (0 and 20 wt% NaCl), followed by stirring overnight. During test, the feed tank was replenished with an equal mass of distillate to maintain constant feed concentration. The permeate flux (J) was calculated according to Eq. (1):

$$J = \frac{W}{A \cdot t} \quad (1)$$

where J (kg·m⁻²·h⁻¹) represents the VMD permeate flux, A (m²) is the effective membrane area (11.94 cm²), and W (kg) denotes the total mass of liquid collected on the permeate side over time t (h).

The salt rejection rate R (%) is calculated using Eq. (2):

$$R = \left(1 - \frac{C_p}{C_f}\right) \times 100\% \quad (2)$$

where C_p , C_f (μS·cm⁻¹) are conductivity of feed and permeate, respectively.

The deep-concentration test was initiated with a 10 wt% NaCl feed solution, where permeate was collected hourly for mass and conductivity measurements without feed replenishment. The experiment continued until the permeate flux stabilized at a constant value, marking the endpoint of the concentration process.

The membrane MDC performance was evaluated using the experimental setup shown in Fig. 1 by incorporating a crystallization tank into the feed circulation loop. The cooling water temperature was maintained at 1°C while using a saturated NaCl solution at 25°C as the feed. After an operation for 1 h, the liquid in the crystallization tank was sampled for observation of crystal formation under an optical microscope (ML31). Following the test, the crystals in the crystallization tank were collected by filtration and dried in an oven at 60°C. X-Ray diffraction (XRD) analysis of collected crystals and commercial NaCl crystals were carried out using RIGAKU MiniFlex600 diffractometer.

3. Results and discussion

3.1. Preparation of SDS composite membranes and VMD performance

The SDS hydrophobic composite membrane was fabricated from the previously synthesized SDS block copolymer via selective swelling. During selective swelling, *n*-hexane selectively permeated into the

PDMS domains due to their strong affinity, causing PDMS expansion. Meanwhile, the rigid PS domains underwent plastic deformation under compression. Subsequent solvent evaporation induced PDMS chain collapse, forming interconnected pores.

The morphology of the SDS composite membrane after swelling was characterized by SEM, with surface porosity and pore diameter statistically analyzed (Fig. 2 and Table S1). As shown in Fig. 2, as-prepared SDS membrane surface primarily consisted of densely isolated circular pores and elongated pores, while the cross-section exhibited well-connected bi-continuous pore structure. The surface porosity was approximately 9.2% with an average pore size of 24.5 nm, whereas the overall porosity reached 50.2%. This discrepancy between surface and volume porosity arose from asynchronous swelling between the surface and bulk. Due to the extremely low surface energy of PDMS (20.4 mN·m⁻¹), it tended to migrate toward the surface during swelling, resulting in lower surface porosity compared to the bulk after swelling [30]. The enrichment of PDMS on the surface endowed the SDS membrane with excellent intrinsic hydrophobicity [31]. The SDS membrane exhibited a water contact angle of 120.5° and a liquid entry pressure (LEP) of 4.4 bar, conclusively demonstrating its excellent anti-wetting capability.

In our previous work, we systematically investigated the MD performance of SDS composite membranes in treating a 3.5 wt% NaCl feed solution. The results demonstrated that the small pore size endowed the SDS membrane with excellent anti-wetting properties, while the high volume porosity formed by selective swelling maintained the high permeate flux. However, apart from membrane wetting issues, the continuous concentration of feed solution during MD inevitably leads to scaling. This scaling phenomenon, characterized by the deposition of non-volatile matter on membrane surfaces and within pore channels, usually causes significant deterioration in both flux and rejection performance. During high-salinity wastewater treatment, scaling primarily occurs through two mechanisms: (1) homogeneous nucleation (crystal formation in bulk solution followed by deposition on membrane surfaces) and (2) heterogeneous nucleation (direct crystal formation on membrane surfaces). The risk of scaling becomes substantially aggravated with the increase of the salinity of MD feed solution [13]. Conventional MD membranes typically feature microporous structures with pore sizes ranging from 0.1 to 1 μm [5]. Even with surface modification like superhydrophobic treatment, these membranes still inevitably suffer from flux decline due to the scaling during operation. Both theoretical and experimental studies have confirmed that membranes with low surface porosity and reduced pore size can significantly mitigate performance decline caused by scaling.

The performance of the SDS membrane was first evaluated using saline solutions with concentrations ranging from 3.5 to 20 wt% to

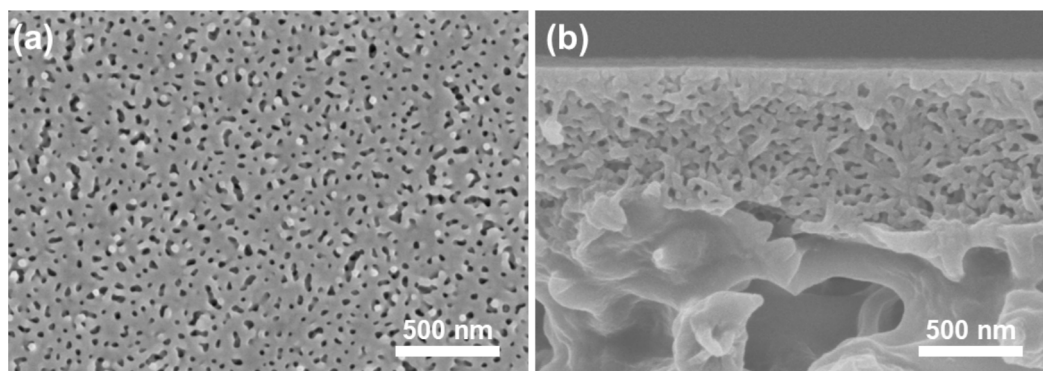


Fig. 2. (a) Surface and (b) cross-section SEM images of the SDS composite membrane by selective swelling in *n*-hexane for 1 h at 25°C.

simulate high-salinity wastewater under constant feed concentration conditions. As shown in Fig. 3a, the permeate flux of the SDS membrane exhibited a decreasing trend with increasing feed salinity. When the MD process was performed using a 3.5 wt% NaCl solution with a feed temperature of 70°C, the membrane demonstrated excellent MD performance with a high flux of $26.0 \text{ kg}\cdot\text{m}^{-2}\cdot\text{h}^{-1}$ while maintaining salt rejection above 99.99%. When the NaCl concentration increased to 5 wt%, the flux slightly decreased to $21.9 \text{ kg}\cdot\text{m}^{-2}\cdot\text{h}^{-1}$ while the desalination performance remained above 99.99%. Further increasing the feed concentration to 10, 15, and 20 wt% resulted in gradual flux reduction to 12.9, 8.7 and $5.2 \text{ kg}\cdot\text{m}^{-2}\cdot\text{h}^{-1}$, respectively. The flux decline from 3.5 to 20 wt% NaCl was attributed to reduced vapor pressure differences. Increasing NaCl concentration decreases solution saturation vapor pressure, thereby weakening the mass transfer driving force [32]. Notably, the flux remained stable during an 8-h test across all salinity levels (Fig. S1).

To confirm that flux reduction resulted from vapor pressure changes rather than scaling, a prolonged 48-h test was conducted using the 20 wt% NaCl solution as the feed. As shown in Fig. 3b, the flux consistently maintained at $5.2 \pm 0.1 \text{ kg}\cdot\text{m}^{-2}\cdot\text{h}^{-1}$ while the salt rejection sustained $> 99.99\%$, aligning with the 8-h test results. This conclusively demonstrated that the flux reduction during VMD was caused by decreased vapor pressure driving force rather than membrane scaling.

Surface pore structure (Fig. S2) and hydrophobicity (Fig. S3) of the SDS membrane after exposure to NaCl solutions with varied concentrations were characterized to assess scaling behaviour. The SEM images revealed only sparse, isolated solid particles distributed on membrane surfaces, with no formation of continuous scaling layers. The porous membrane structure remained intact and well-defined after test. WCA measurements demonstrated negligible hydrophobicity loss after 8 h of operation across all salinity levels, showing $\leq 3.5^\circ$ decline (from 120.5° to 117.0°) even after an 8-h test with the 20 wt% saline feed. This minimal reduction in WCA confirmed the outstanding wetting resistance

and stable performance of the SDS membrane under high-salinity conditions. These results collectively verified that the SDS membrane effectively resisted salt-induced scaling contamination, preserving its structural integrity and surface properties even under high-salinity conditions.

3.2. Anti-scaling performance of the SDS membrane

In the performance evaluation under different salt concentrations, deionized water was replenished into the feed solution during testing to maintain a constant feed concentration. This operational condition may somewhat mitigate the actual scaling during real operation. We further conducted MD deep-concentration experiments for hypersaline water (10 wt% NaCl) to evaluate the comprehensive performance of the SDS membrane. As shown in Fig. 4, at the beginning of the concentration test with 10 wt% feed solution, the SDS composite membrane exhibited an initial flux of $13.4 \text{ kg}\cdot\text{m}^{-2}\cdot\text{h}^{-1}$, consistent with the flux obtained under constant concentration testing ($12.9 \text{ kg}\cdot\text{m}^{-2}\cdot\text{h}^{-1}$). However, the flux gradually declined as the feed solution became progressively concentrated. When NaCl concentrations reached 15 wt% and 20 wt%, the corresponding fluxes decreased to $9.0 \text{ kg}\cdot\text{m}^{-2}\cdot\text{h}^{-1}$ and $6.8 \text{ kg}\cdot\text{m}^{-2}\cdot\text{h}^{-1}$ respectively, which was aligning with constant-concentration experimental results. Upon reaching supersaturated conditions ($>30 \text{ wt}\%$), the flux stabilized at $4.8 \text{ kg}\cdot\text{m}^{-2}\cdot\text{h}^{-1}$. Throughout the deep-concentration process from 10 wt% to 30 wt%, the flux decreased from $13.4 \text{ kg}\cdot\text{m}^{-2}\cdot\text{h}^{-1}$ to $4.8 \text{ kg}\cdot\text{m}^{-2}\cdot\text{h}^{-1}$, representing an overall reduction of approximately 64.2%. The decline in flux primarily resulted from decreased saturation vapor pressure caused by the increase in salt concentration. Under supersaturated feed conditions, the membrane maintained stable flux while visible crystal formation was observed in the feed tank. This flux stabilization likely reflected a dynamic equilibrium where crystal precipitation maintains constant liquid-phase salt concentration, preventing further reduction in saturation vapor

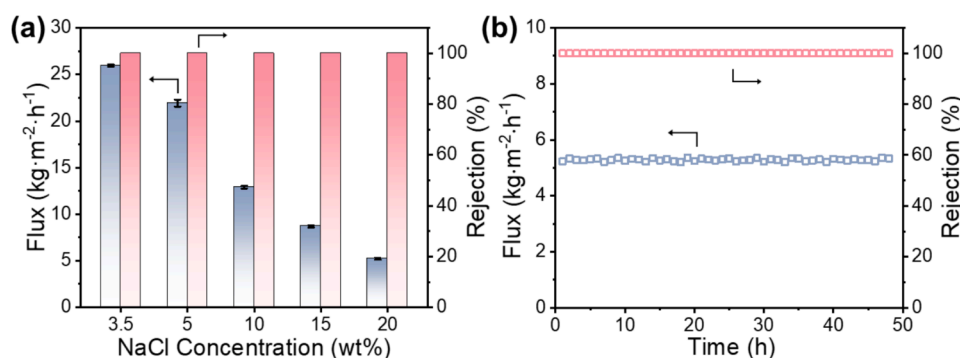


Fig. 3. (a) VMD performance of the SDS membrane using NaCl solutions with different concentrations. (b) VMD performance of the SDS membrane with the 20 wt% NaCl solution for 48 h.

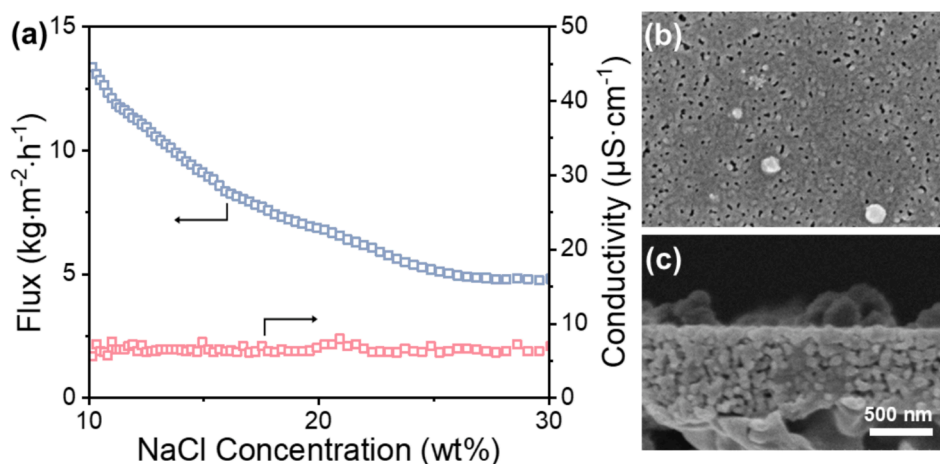


Fig. 4. (a) Flux and distillate conductivity of the SDS membrane during the MD concentration process. (b) surface and (c) cross-section SEM images after concentration process. (b) has the same magnification as the scale bar shown in (c).

pressure. Throughout the concentration process, the permeate conductivity remained $< 10 \mu\text{S}\cdot\text{cm}^{-1}$, meeting the purified water standards, confirming that increased salinity had negligible impact on the rejection performance of the SDS ultrafiltration membrane.

SEM images (Fig. 4b-c) showed that only a very small amount of irregular white particles could be observed on the SDS membrane surface after the deep-concentration test. Although prolonged operation resulted in some reduction of surface pores and a slight decrease in surface porosity to 7.9%, the morphological changes of surface pore channels were minimal. The cross-section maintained well-defined bicontinuous pore structure, indicating that long-term high-temperature (70°C) operation had little effect on the membrane structure. EDS elemental mapping results of the tested membrane surface and cross-section (Fig. S4) showed extremely low Na and Cl content (less than 1 wt%). Both SEM and EDS results demonstrated that no scaling occurred on the SDS membrane after the concentration test, confirming the excellent anti-scaling performance of the SDS membrane.

In practical systems, feed solutions often contain various contaminants, notably including surfactants (such as sodium dodecyl sulfate) and inorganic foulants (CaSO₄) [33]. Previous work has demonstrated that the SDS membrane maintain excellent stability even when treating saline systems containing surfactants, showing stable performance over a 156-h test period [27]. Inorganic foulants and surfactants exhibit different fouling mechanisms: surfactants selectively adhere to hydrophobic surfaces and convert them from hydrophobic to hydrophilic and leading to membrane wetting [34]. In contrast, inorganic pollutants are more prone to precipitate under supersaturated conditions near the membrane surface with the water evaporation during MD and significantly increasing scaling risks, which is due to the low solubility of inorganic pollutants and further decreases with rising temperatures [35].

In this study, the 20 wt% NaCl solution containing saturated CaSO₄ was chosen as the typical high-salinity wastewater to evaluate the anti-scaling performance of the SDS membrane. As shown in Fig. 5, the SDS composite membrane exhibited outstanding stability throughout the a 24-h operation: the flux remained consistently around $4.2 \text{ kg}\cdot\text{m}^{-2}\cdot\text{h}^{-1}$ while salt rejection maintained above 99.99%. SEM results indicated that after a continuous operation of 24 h, the nanoporous structure of the SDS membrane surface remained intact, with no observed CaSO₄ scaling or crystal accumulation (Fig. S5). Cross-sectional morphology analysis further confirmed the undamaged membrane structure, with well-maintained nanoporous channels, indicating excellent anti-scaling performance. Additionally, the scaling resistant of the SDS membrane to CaSO₄-saturated solution without NaCl (0 wt%) was also investigated and shown in Fig. S6 to avoid the influence of NaCl concentration on the

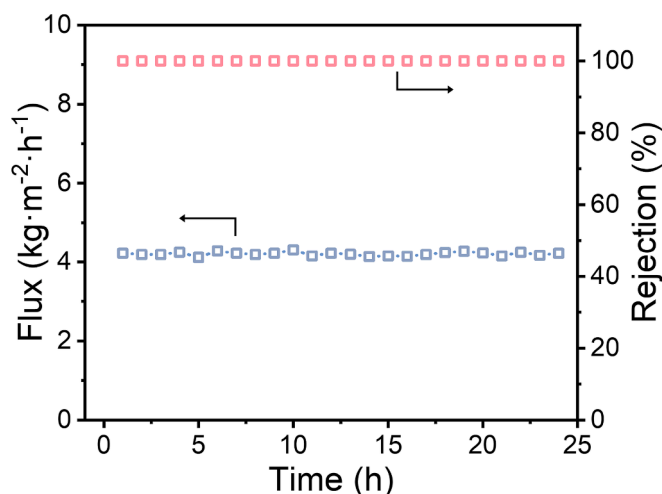


Fig. 5. VMD performance of the SDS membrane for the treatment of 20 wt% NaCl solution containing saturated CaSO₄.

solubility of CaSO₄. During a 24-h test, the permeate flux remained consistently at approximately $27.8 \text{ kg}\cdot\text{m}^{-2}\cdot\text{h}^{-1}$ for the first 10 h and gradually decreased to $\sim 25.5 \text{ kg}\cdot\text{m}^{-2}\cdot\text{h}^{-1}$. Besides, the conductivity of the permeate simultaneously raised slightly after 10 h, but still maintained below $10 \mu\text{S}\cdot\text{cm}^{-1}$. After a 24-h continuous operation, the flux of saturated CaSO₄ system showed a modest flux decline of 8.3% while that with 20 wt% NaCl remained stable. The stability observed in high-salinity environments is benefited from the suppression of NaCl on CaSO₄ precipitation [36]. Therefore, despite the NaCl concentration may have some influence on the scaling behavior of CaSO₄ in MD, the SDS membrane maintained relatively stable flux performance compared to other membranes. Such minimal flux reduction demonstrated the excellent anti-scaling properties of the SDS membrane even under rigorous CaSO₄-saturated conditions.

The outstanding anti-scaling performance of the SDS membrane was attributed to its optimized structural characteristics. The small pore size and surface porosity, coupled with the smooth membrane surface which, effectively prevent physical attachment of gypsum crystals formed through homogeneous nucleation, thereby limiting crystal accumulation on the membrane surface [37,38]. Compared to other micro-filtration MD membranes in literature, the SDS ultrafiltration membrane exhibited superior anti-scaling properties and long-term stabilities in processing of high-salinity wastewater (Table S2).

According to the classical nucleation theory, membrane surface properties such as hydrophobicity and porosity play a critical role in governing heterogeneous nucleation behavior [39]. The formation of crystals requires overcoming the Gibbs free energy barrier (ΔG^*), which differs between homogeneous nucleation in bulk solution and heterogeneous nucleation on the membrane surface. While the Gibbs free energy for homogeneous nucleation ($\Delta G_{\text{homogeneous}}^*$) in bulk solution can be calculated using conventional equation, the potential of heterogeneous surface nucleation can be deduced from $\Delta G_{\text{homogeneous}}^*$ by incorporating membrane properties including hydrophobic and surface porosity calculated as the following equation [40],

$$\Delta G_{\text{heterogeneous}}^* = \Delta G_{\text{homogeneous}}^* \left[\frac{1}{4} (2 + \cos\theta)(1 - \cos\theta)^2 \right] \left[1 - \varepsilon \frac{(1 + \cos\theta)^2}{(1 - \cos\theta)^2} \right]^3 \quad (3)$$

where θ is the apparent contact angle between the solution and membrane, and ε is the surface porosity of the membrane.

According to the equation above, a lower surface porosity and a higher contact angle of the membrane result a lower scaling tendency because of the higher requirement of free energy for heterogeneous nucleation. The low surface porosity (9.2%) and moderate hydrophobicity (120.3°) of the SDS membrane rendered the membrane with a high energy barrier for heterogeneous nucleation.

Additionally, the smooth surface morphology of the SDS ultrafiltration membrane compared to conventional MD membranes significantly reduced available nucleation sites, thereby suppressing heterogeneous nucleation at the membrane surface [31,41,42]. The SDS ultrafiltration membrane showed an average pore size of 24.5 nm, which was significantly smaller than typical crystal dimensions. This size difference effectively restricted intra-pore crystal growth and preserved pore structural integrity [22]. Furthermore, the excellent wetting resistance (a LEP value of 4.4 bar) prevented partial pore wetting [5,6]. This barrier effect blocked feed solution penetration into pore channels, further minimizing risks of intra-pore crystal formation and growth [14]. These synergistic effects enabled the SDS membrane to maintain long-term stability even under severe scaling-prone conditions in MD systems. Therefore, the SDS membrane combined superior anti-wetting and anti-scaling properties. Notably, visible NaCl crystal precipitation observed during hypersaline concentration tests confirmed its strong potential for MDC applications.

3.3. Performance of MDC

MDC represents a promising technology combining MD with crystallization, capable of simultaneous water and salt/mineral resource recovery. This integrated approach proves particularly suitable for high-salinity wastewater treatment, providing an effective pathway toward zero liquid discharge. The above results demonstrated that the SDS ultrafiltration membrane prepared by selective swelling exhibited stable MD performance at high-salinity environments with excellent anti-scaling properties, and no scaling blockage was observed on the membrane surface after testing. Besides, white crystal precipitation was visibly formed in the feed tank upon completing the deep-concentration experiments, indicating the potential applicability in MDC processes.

Therefore, the MDC performance of the SDS membrane was assessed using a saturated saline solution prepared at 25°C as the crystallization mother liquor.

The MDC process was achieved by integrating a crystallization unit with the MD system. The flux and rejection performance throughout the process were shown in Fig. 6. During the long-term MDC test (168 h), the SDS membrane maintained a stable flux of $\sim 3.0 \text{ kg}\cdot\text{m}^{-2}\cdot\text{h}^{-1}$. The rejection performance of the SDS membrane was above 99.99% during the whole long-term test with the permeate conductivity below 15

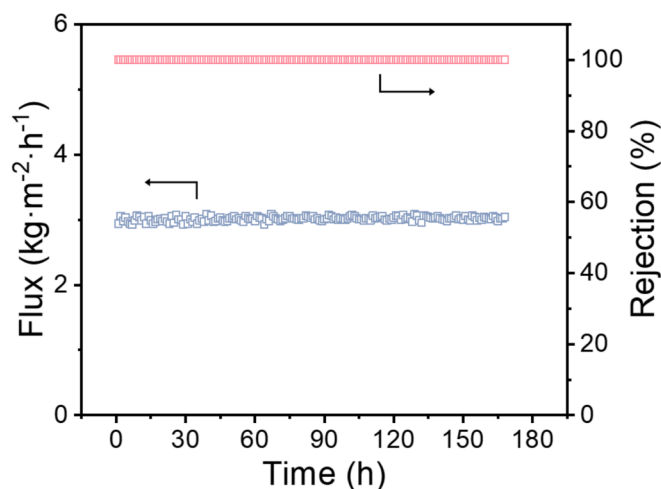


Fig. 6. MDC performance of the SDS membrane with the saturated NaCl solution as crystallization mother liquor.

$\mu\text{S}\cdot\text{cm}^{-1}$ (Fig. S7). No sudden increases or decreases in flux were observed throughout the experiment, demonstrating the excellent stability of the SDS membrane under prolonged supersaturated conditions. However, compared to the standalone MD process ($4.8 \text{ kg}\cdot\text{m}^{-2}\cdot\text{h}^{-1}$ under supersaturated conditions), the flux decreased slightly. This reduction primarily stemmed from the temperature drop in the overall circulation system caused by the introduction of the crystallization unit, which consequently reduced the mass transfer driving force. In the MDC process, the feed solution entered the low-temperature crystallization unit after treating in the MD unit. This rapid temperature drop promoted the crystallization process, simultaneously lowered the feed solution temperature and thus the saturation vapor pressure, ultimately resulting in a slight decrease in membrane flux.

During MDC process, water evaporation near the membrane surface created localized supersaturated conditions. Although this environment may potentially increase scaling risks, it significantly promotes the nucleation and growth of crystals at the same time. Compared to conventional crystallization processes, MDC demonstrates higher nucleation rates and shorter induction periods [37,38]. The SDS membrane, with its unique surface characteristics (specifically the smaller pore size and relatively smooth surface structure compared to microfiltration membranes), effectively suppressed both homogeneous nucleation deposition and heterogeneous nucleation on membrane surfaces. Even when limited crystal nuclei formed on the membrane surface, the smooth surface and small pore size enabled these nuclei to detach from the membrane surface under fluid shear forces and re-entered the circulation system. This mechanism ensured stable membrane flux throughout the entire operation process [11].

Optical microscopy observations in Fig. 7a revealed the formation of well-defined, regularly shaped cubic NaCl crystals measuring $34.1 \pm 8.1 \mu\text{m}$ in the feed solution within the operation time of 1 h. The crystal size was significantly larger than the pore size of the SDS membrane ($24.5 \pm 1.3 \text{ nm}$), this size disparity provided strong evidence that the small pore structure effectively suppressed intra-pore crystallization. This rapid crystallization process could be attributed to the highly concentrated feed solution and the introduction of the crystallization unit in MD process. After a continued operation for 5 h, precipitated white crystals became clearly visible in the crystallization tank (Fig. 7b). The formed crystals conclusively demonstrate the remarkable advantages MDC system in promoting salt crystallization while simultaneously validating the potential of the SDS membrane for this hybrid process. After test, the crystals were recovered through filtration to remove excess mother liquor, followed by overnight drying at 60°C . Thus-obtained white granular crystals were collected and shown in Fig. 7c. Besides, SEM



Fig. 7. (a) Crystal morphology observed under an optical microscope after 1 h of MDC; (b) white crystals formed in the crystallization tank during MDC. (c) The crystal salt after drying.

images of those crystals showed slightly irregular morphologies (Fig. S9a-b), which may be attributed to the complex crystallization environment, including rapid nucleation under supersaturated conditions and quenching effects. More importantly, the XRD analysis confirmed that the recovered NaCl crystals (Fig. S9c) matched the standard diffraction pattern of commercial NaCl, indicating high crystallinity and purity."

The surface scaling behavior of the SDS membrane after MDC test was characterized using SEM and EDS (Fig. S8, S10, and Table S3). From Fig. S8a-b, only sparse particulate matter was visible on the SDS composite membrane surface under low-magnification SEM observation, with no evidence of continuous salt crystal accumulation. The microporous PVDF substrate in the membrane cross-section maintained intact pore structures without any crystal-induced damage. High-magnification imaging revealed clearly defined surface pore channels completely free from scaling blockage, while the cross-sectional pore architecture remained stable even after 168 h of continuous supersaturated saline exposure (Fig. S8c-d). EDS analysis further confirmed these findings. Low-magnification examination showed smooth membrane surfaces devoid of crystalline deposits. Although EDS mapping detected trace Na and Cl signals, their surface concentrations remained below 1 wt%, quantitatively confirming minimal salt deposition (Fig. S10 and Table S3). These comprehensive results demonstrated the exceptional performance and long-term stability of the SDS ultrafiltration membrane in MDC.

The experimental results strongly support that homogeneous nucleation predominates in our system, demonstrating the effective scaling resistance mechanism of SDS membranes through surface heterogeneous crystallization suppression. Three key findings support this conclusion: (1) the stable flux behavior during treatment of saturated brine solutions suggested minimal surface blockage, which would be expected for heterogeneous nucleation [11]; (2) the broad size distribution and irregular morphology of the obtained crystals (Fig. S9) differed markedly from the uniform crystals typically produced by surface-controlled heterogeneous nucleation; and (3) post-test membrane examination revealed only minimal crystal deposition on the membrane surface, indicating that crystallization mostly occurred in the bulk solution rather than at the membrane interface [43]. The tailored surface properties of the SDS membrane created thermodynamically unfavorable conditions for heterogeneous nucleation while maintaining optimal vapor transport, providing a robust solution for hypersaline wastewater treatment.

4. Conclusion

In this work, the hydrophobic SDS ultrafiltration membrane fabricated via selective swelling was successfully employed for MD desalination of high-salinity brines. The membrane demonstrated stable flux performance across various salinity levels (5–20 wt%), with flux reduction observed at higher concentrations while maintaining consistent operational stability. The membranes exhibited remarkable

stability during an extended 48-h test with 20 wt% NaCl feed solution, maintaining a constant flux of $5.2 \pm 0.1 \text{ kg}\cdot\text{m}^{-2}\cdot\text{h}^{-1}$ while achieving permeate conductivity below $10 \mu\text{S}\cdot\text{cm}^{-1}$, thus illustrating the outstanding performance in hypersaline membrane distillation. In systems containing saturated CaSO_4 as the inorganic contaminant, the membrane maintained stable flux throughout a 24-h continuous operation, no observable scaling or crystal accumulation on membrane surfaces in post-test characterization. When implemented in MDC systems using saturated NaCl as the crystallization mother liquor, the SDS ultrafiltration membrane exhibited stable flux and salt rejection (>99.99%) during continuous operation exceeding 160 h, without any scaling or wetting phenomena. The successful observation of salt crystal formation and production of both high-purity water and crystalline products demonstrated the successful application of the SDS membrane in MDC. This work presents new insights for developing high-performance, scaling-resistant membranes for advanced membrane distillation applications, particularly highlighting the effectiveness of reduced pore size for enhancing anti-wetting and anti-scaling performance.

Declaration of competing interest

The authors declare that they have no known competing financial interests or personal relationships that could have appeared to influence the work reported in this paper.

Acknowledgement

This work was financially supported by the National Key Research and Development Program of China (2024YFE0112300).

Appendix A. Supplementary data

Supplementary data to this article can be found online at <https://doi.org/10.1016/j.seppur.2025.133614>.

References

- [1] S. Du, P. Zhao, L. Wang, G. He, X. Jiang, Progresses of advanced anti-fouling membrane and membrane processes for high salinity wastewater treatment, *Results Eng.* 17 (2023) 100995.
- [2] K.M. Shah, L.H. Billinge, X. Chen, H. Fan, Y. Huang, R.K. Winton, N.Y. Yip, Drivers, challenges, and emerging technologies for desalination of high-salinity brines: a critical review, *Desalination* 538 (2022) 115827.
- [3] A. Shokri, M. Sanavi Fard, Corrosion in seawater desalination industry: A critical analysis of impacts and mitigation strategies, *Chemosphere* 307 (2022) 135640.
- [4] E.J. Okampo, N. Nwulu, Optimisation of renewable energy powered reverse osmosis desalination systems: a state-of-the-art review, *Renew. Sustain. Energy Rev.* 140 (2021) 110712.
- [5] M. Qasim, I.U. Samad, N.A. Darwish, N. Hilal, Comprehensive review of membrane design and synthesis for membrane distillation, *Desalination* 518 (2021) 115168.
- [6] S. Yang, S. Abdalkareem, D. Bokov, S. Chupradit, A. Taghvaie, A.S. El-shafay, Membrane distillation technology for molecular separation: a review on the fouling, wetting and transport phenomena, *J. Mol. Liq.* 349 (2021) 118115.

- [7] L. Jiao, K. Yan, J. Wang, S. Lin, G. Li, F. Bi, L. Zhang, Low surface energy nanofibrous membrane for enhanced wetting resistance in membrane distillation process, *Desalination* 476 (2020) 114210.
- [8] X. Dai, Q. Wei, Y. Wang, Q. Li, S. Cui, Z. Nie, A novel strategy to enhance the desalination stability of FAS (fluoroalkylsilane)-modified ceramic membranes via constructing a porous SiO₂@PDMS (polydimethylsiloxane) protective layer on their top, *Chem. Eng. J.* 435 (2022) 134757.
- [9] R. Sarbatly, C.-K. Chiam, Evaluation of geothermal energy in desalination by vacuum membrane distillation, *Appl. Energy* 112 (2013) 737–746.
- [10] S.T. Bouguecha, S.E. Aly, M.H. Al-Beiruty, M.M. Hamdi, A. Boubakri, Solar driven DCMD: performance evaluation and thermal energy efficiency, *Chem. Eng. Res. Des.* 100 (2015) 331–340.
- [11] J. Pan, M. Chen, X. Xu, S.-P. Sun, Z. Wang, Z. Cui, W. Xing, N. Tavajohi, Enhanced anti-wetted PVDF membrane for pulping RO brine treatment by vacuum membrane distillation, *Desalination* 526 (2022) 115533.
- [12] L. Eykens, I. Hitsov, K. De Sitter, C. Dotremont, L. Pinoy, I. Nopens, B. Van der Bruggen, Influence of membrane thickness and process conditions on direct contact membrane distillation at different salinities, *J. Membr. Sci.* 498 (2016) 353–364.
- [13] H. Liu, K.I. Jacob, Y. Wang, Scaling in membrane distillation (MD): Current state of art insight on mechanisms and Membrane design, *Desalination* 581 (2024) 117539.
- [14] S. Xie, N.H. Wong, J. Sunarso, Q. Guo, C. Hou, Z. Pang, Y. Peng, Gypsum scaling mechanisms on hydrophobic membranes and its mitigation strategies in membrane distillation, *J. Membr. Sci.* 648 (2022) 120297.
- [15] P. Wang, W. Cheng, X. Zhang, J. Li, J. Ma, T. Zhang, Engineering a protective surface layer to resist membrane scaling and scale-induced wetting in membrane distillation for the treatment of hypersaline wastewater, *Chem. Eng. J.*, 452 (2023) 139167.
- [16] Y. Liao, G. Zheng, J.J. Huang, M. Tian, R. Wang, Development of robust and superhydrophobic membranes to mitigate membrane scaling and fouling in membrane distillation, *J. Membr. Sci.* 601 (2020) 117962.
- [17] Z. Zhu, G. Tan, D. Lei, Q. Yang, X. Tan, N. Liang, D. Ma, Omniphobic membrane with process optimization for advancing flux and durability toward concentrating reverse-osmosis concentrated seawater with membrane distillation, *J. Membr. Sci.* 639 (2021) 119763.
- [18] P. Zhang, S. Xiang, R.R. Gonzales, Z. Li, Y.-H. Chiao, K. Guan, M. Hu, P. Xu, Z. Mai, S. Rajabzadeh, K. Nakagawa, H. Matsuyama, Wetting-and scaling-resistant superhydrophobic hollow fiber membrane with hierarchical surface structure for membrane distillation, *J. Membr. Sci.* 693 (2024) 122338.
- [19] C. Wang, L. Liu, Y. Wang, P. Hou, J. Wang, J. Wang, Treatment of various saline wastewaters by membrane distillation with omniphobic polyvinyl alcohol membrane, *Desalination* 591 (2024) 118011.
- [20] G. Tan, D. Xu, Z. Zhu, X. Zhang, J. Li, Tailoring pore size and interface of superhydrophobic nanofibrous membrane for robust scaling resistance and flux enhancement in membrane distillation, *J. Membr. Sci.* 658 (2022) 120751.
- [21] T. Horseman, C. Su, K.S.S. Christie, S. Lin, Highly effective scaling mitigation in membrane distillation using a superhydrophobic membrane with gas purging, *Environ. Sci. Technol. Lett* 6 (2019) 423–429.
- [22] M. Gryta, Influence of polypropylene membrane surface porosity on the performance of membrane distillation process, *J. Membr. Sci.*, 287 (2007) 67–78.
- [23] K. Miao, Y. Song, K. Guan, J. Liu, H. Matsuyama, D. Zou, Z. Zhong, Robust hydrophobic ceramic membrane for high-salinity wastewater separation via membrane distillation, *Desalination* 592 (2024) 118091.
- [24] A.B. Yeszhanov, I.V. Korolkov, O. Güven, G.B. Melnikova, S.S. Dosmagambetova, A.N. Borissenko, A.K. Nurkassimov, M.T. Kassymzhanov, M.V. Zdorovets, Effect of hydrophobized PET TeMs membrane pore-size on saline water treatment by direct contact membrane distillation, *RSC Adv.*, 14 (2024) 4034–4042.
- [25] Y. Choi, L. Suu, J. Lim, J.-S. Choi, Recovery of lithium carbonate crystals from a high salinity solution using membrane crystallizer with concentration and temperature gradients, *Desalination* 594 (2025) 118311.
- [26] W.N.A. Wan Osman, N.I. Mat Nawi, S. Samsuri, M.R. Bilad, Y. Wibisono, E. Hernández Yáñez, J. Md Saad, A review on recent progress in membrane distillation crystallization, *ChemBioEng Rev.* 9 (2022) 93–109.
- [27] Z. Li, S. Qiu, X. Ying, F. Zhang, X. Xu, Z. Cui, Y. Wang, Nanoporous thin films of hydrophobic block copolymers enabled by selective swelling for membrane distillation, *J. Membr. Sci.* 679 (2023) 121710.
- [28] L. Leibler, Theory of microphase separation in block copolymers, *Macromolecules* 13 (1980) 1602–1617.
- [29] J. Zhou, Y. Wang, Selective swelling of block copolymers: an upscaleable greener process to ultrafiltration membranes? *Macromolecules* 53 (2019) 5–17.
- [30] A.F. Putranto, C. Petit-Etienne, S. Cavalaglio, B. Cabannes-Boué, M. Panabiere, G. Forcina, G. Fleury, M. Kogelschatz, M. Zelsmann, Controlled anisotropic wetting by plasma treatment for directed self-assembly of high- γ block copolymers, *Appl. Mater. Interfaces* 16 (2024) 27841–27849.
- [31] S. Qiu, Z. Li, X. Ye, X. Ying, J. Zhou, Y. Wang, Selective Swelling of Polystyrene (PS)/ Poly (dimethylsiloxane) (PDMS) Block Copolymers in Alkanes, *Macromolecules* 56 (2023) 215–225.
- [32] M. Safavi, T. Mohammadi, High-salinity water desalination using VMD, *Chem. Eng. J.*, 149 (2009) 191–195.
- [33] Y. Wang, J. Liu, Z. Li, X. Liu, W. Li, Revisiting scaling of calcium sulfate in membrane distillation: uncertainty of crystal-membrane interactions, *Water Res.*, 239 (2023) 120060.
- [34] E. Guillen-Burrieza, M.O. Mavukkandy, M.R. Bilad, H.A. Arafat, Understanding wetting phenomena in membrane distillation and how operational parameters can affect it, *J. Membr. Sci.* 515 (2016) 163–174.
- [35] K.S.S. Christie, Y. Yin, S. Lin, T. Tong, Distinct behaviors between gypsum and silica scaling in membrane distillation, *Environ. Sci. Technol.* 54 (2020) 568–576.
- [36] J. Song, P. Shi, Y. Wang, M. Jiang, Kinetics study on the effect of NaCl on the CaSO₄ dissolution behavior, *IOP Conf. Ser.: Mater. Sci. Eng.* 301 (2018) 012154.
- [37] Y. Choi, G. Naidu, L.D. Nghiem, S. Lee, S. Vigneswaran, Membrane distillation crystallization for brine mining and zero liquid discharge: opportunities, challenges, and recent progress, *Environ. Sci.: Water Res. Technol.* 5 (2019) 1202–1221.
- [38] Y. Choi, G. Naidu, S. Lee, S. Vigneswaran, Effect of inorganic and organic compounds on the performance of fractional-submerged membrane distillation-crystallizer, *J. Membr. Sci.* 582 (2019) 9–19.
- [39] M. Volmer, A. Weber, Keimbildung in Übersättigten Gebilden 119U (1926) 277–301.
- [40] E. Curcio, E. Fontananova, G. Di Profio, E. Drioli, Influence of the structural properties of poly(vinylidene fluoride) membranes on the heterogeneous nucleation rate of protein crystals, *J. Phys. Chem. B* 110 (2006) 12438–12445.
- [41] S. Meng, Y. Ye, J. Mansouri, V. Chen, Crystallization behavior of salts during membrane distillation with hydrophobic and superhydrophobic capillary membranes, *J. Membr. Sci.* 473 (2015) 165–176.
- [42] N.H. Lin, W.-Y. Shih, E. Lyster, Y. Cohen, Crystallization of calcium sulfate on polymeric surfaces, *J. Colloid Interface Sci.* 356 (2011) 790–797.
- [43] A. Ouda, Y. Bajón-Fernández, E. McAdam, Methods to modify supersaturation rate in membrane distillation crystallisation: control of nucleation and crystal growth kinetics (including scaling), *J. Membr. Sci.*, 691 (2024) 122249.